Characterization of photo-neutrons produced by 150 MeV and 1 GeV electrons impinging on high Z-metallic targets for neutron resonance spectroscopy

ElTayeb ElSaady[1], *Mustafa M. M. ElAshmawy*[1], *Hosnia M. Abu-Zeid*[2], *Afaf A. Nada*[2], *Fatma ElZahraa M. Ragab*[2].

[1] *Egyptian Nuclear and Radiological Regulatory Authority, Cairo, Egypt.*
[2] *Faculty of women for Arts, Sci. and Ed., Ain Shams University, Cairo, Egypt.*

Abstract. Monte Carlo calculations have been performed using MCNP code to study the generation, angular distribution and energy spectrum of photo-neutrons for 1 GeV and 150 MeV electron beam energies impinging on different thickness of Tungsten, Tantalum and Lead targets. It is noticed that the photo-neutron yield increases as the target thickness increases then saturates beyond an optimized thickness of the target. Moreover, the photo-neutron yield shows significant increase as the electron energy increases. At the optimized thickness, the angular distribution of photo-neutrons is found almost isotropic for 150 MeV electrons and anisotropic for 1 GeV electrons. Further, by increasing the electron energy and/or the target thickness the angular distribution is found to be forward peaked. The energy spectrum of photo-neutrons can be well described by a Maxwellian distribution for both electron energies. Such calculations can help in developing a photo-neutron source based time of flight facility (TOF) for elemental and isotopic identification via neutron resonance spectroscopy. Photo-neutron yields, angular distribution, mean energy, energy spectrum and nuclear temperature for 1 GeV and 150 MeV electron energies and different target materials are presented.

1.Introduction

In earlier works, the neutrons produced in reactors or through spallation reaction were mainly used to study the nuclear reactions, measurement of cross sections and elemental analysis in different materials because of their high neutron flux. Electron accelerator based neutron sources proving themselves as an attractive alternative to spallation neutron sources because of their compactness, easy handling, adjustable flux, no radioactive waste, less shielding requirement, etc. Recently low and medium electron accelerators have become very popular to be used for elemental and isotopic identification via neutron resonance spectroscopy ***(Junghans A.; 2014)***.

In the current work, we studied the characterization and optimization of the photo-neutrons produced from the impinging of GeV Class electrons on different metallic targets such as Tungsten (W), Tantalum (Ta) and Lead (Pb) then compared with that produced from

150 MeV electrons. The angular distribution, mean energy, energy spectrum and nuclear temperature of photoneutrons are evaluated.

2.Photo-neutrons production mechanisms

The most common way for producing high gamma fluxes in the Giant Dipole Resonance (GDR) region is the bremsstrahlung process resulting from high energy electrons passing through high Z-materials. This process has a cross section linear with energy above 20 MeV. The resulting bremsstrahlung spectrum is widely spread in the energy range from zero to the incident energy of electron, and only a small fraction of these photons are "useful" photons, i.e. have energy greater than the binding energy of neutron and lying in the GDR range of 15±5 MeV. Therefore, the overall efficiency of neutron production is much lower than one might expect by having in mind the direct photonuclear process ***(Ridikas &et. al.; 2002)***. If the absorbed photon has energy greater than the binding or separation energy of neutron from nucleus, then neutron is emitted. Photonuclear interaction is mainly the result of three specific processes: giant dipole resonance (GDR), quasi-deuteron (QD) production and photo-pion decay. The GDR neutrons are produced by photons with energies from threshold energy to 30 MeV. While at $50 < E < 140$ MeV, the photoneutron production is due to quasi-deuteron effect (QD). Above 140 MeV, photoneutrons are produced via photo-pion production ***(Petwal &et. al.; 2007)***.

3. Monte Carlo MCNP calculations

By using LA150U photonuclear library in Monte Carlo MCNP code, the photonuclear physics has been introduced with photon energies up to150 MeV ***(X-5 MCNP Team; 2003) (Quintieri L. & et al.;2012)***. In the current study, F_1 and F_5 tally are used for scoring photo neutrons yield and fluence in different angels. 10^6-10^7 histories are run to reduce statistical error less than 5%. Since Monte Carlo MCNP calculations depend sensitively on the simulation geometry, the current simulation results was compared with published data ***(Swanson W. P.; 1979) (Petwal V. C. & et al.; 2007)*** to check the photonuclear physics contained in the code. Figure 1 shows the comparison between the current simulation results and the published data for cylindrical lead target (Pb-207) (thickness 1.68 cm and radius 3 cm), for which measured data are available**.**

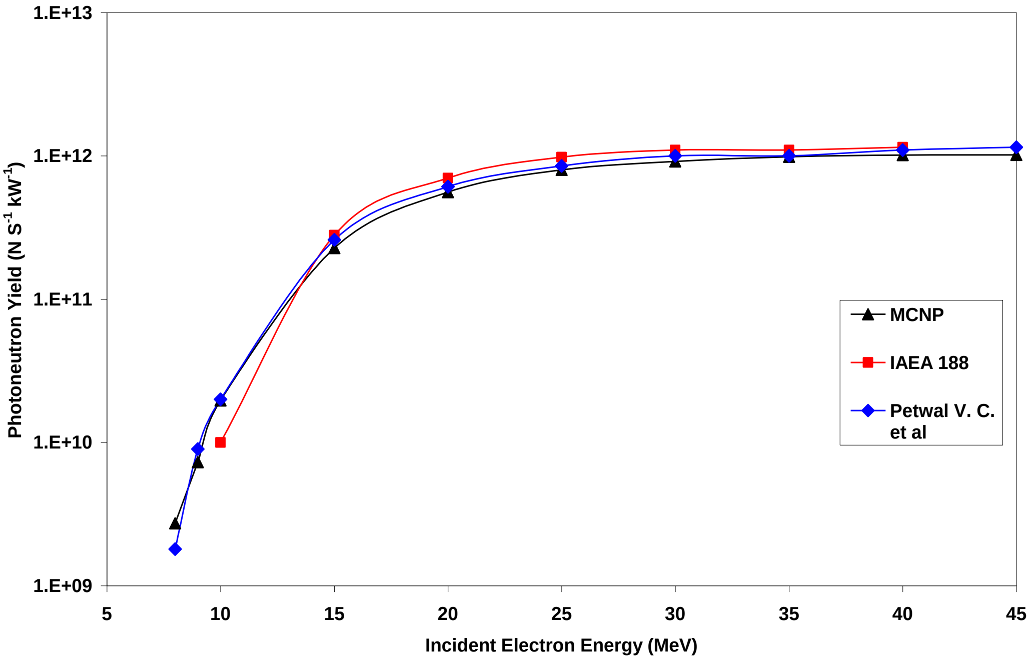

Figure 1: the photonuclear yield per kW produced from Lead (Pb-207) target (1.68 cm thickness, r=3cm) bombarded to different electron energies.

It is clearly concluded from figure 1 that the current simulation results for Lead (pb-207) show good agreement with the published data.

3.1 Photo-neutron yield

Photoneutron yield (neutron/s) is calculated for different target thickness and for different electron beam energies by using the following formula ***(Petwal &et. al.; 2007) (Zolfaghari M. and Sedaghatizadeh M.; 2015)***:

$$\varphi_n = \frac{N_0 \rho t \sigma_t(E)}{M} \varphi_e \qquad (1)$$

Here M, ρ and t are the atomic mass, density and target thickness respectively. N_0 is the Avogadro number, φ_e is the incident electron fluence rate (electron/s), $\sigma_t(E)$ is the total photonuclear cross-section (the sum of all cross-sections that leads to neutron emission) and E is the electron incident energy. Figure 2 shows the neutron yield as function of target thickness for 1 GeV electron beam impinging on Tungsten, Tantalum and Lead targets respectively. Figure 3 shows the neutrons yield produced from 1GeV and 150 MeV electron energies impinging on Tungsten target.

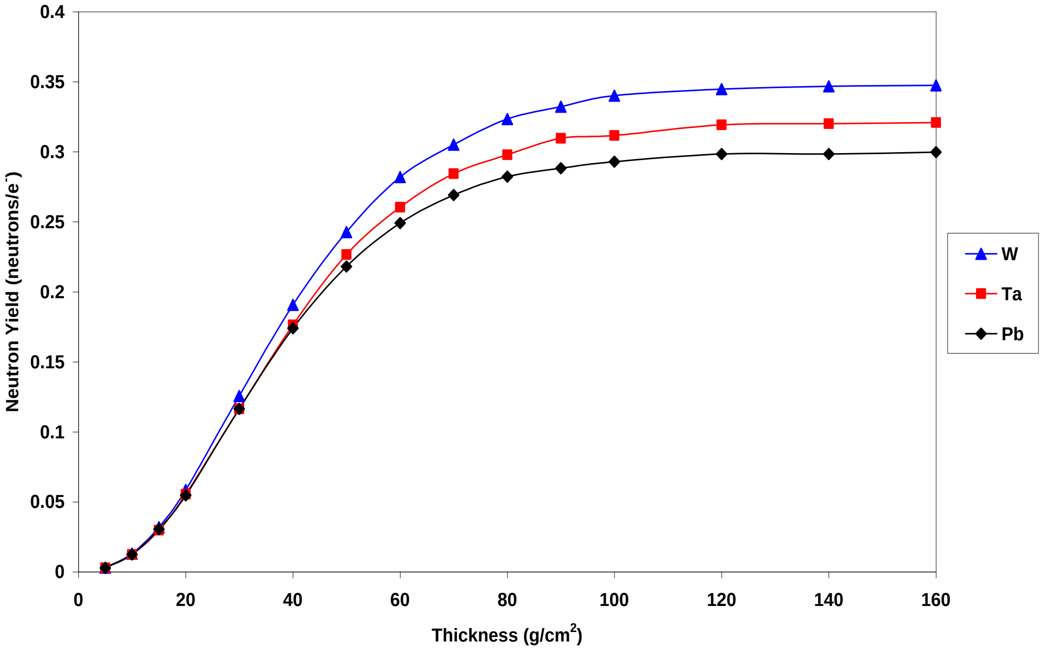

Figure2: Neutron yield as function of target thickness for 1 GeV energy electron incident on different targets.

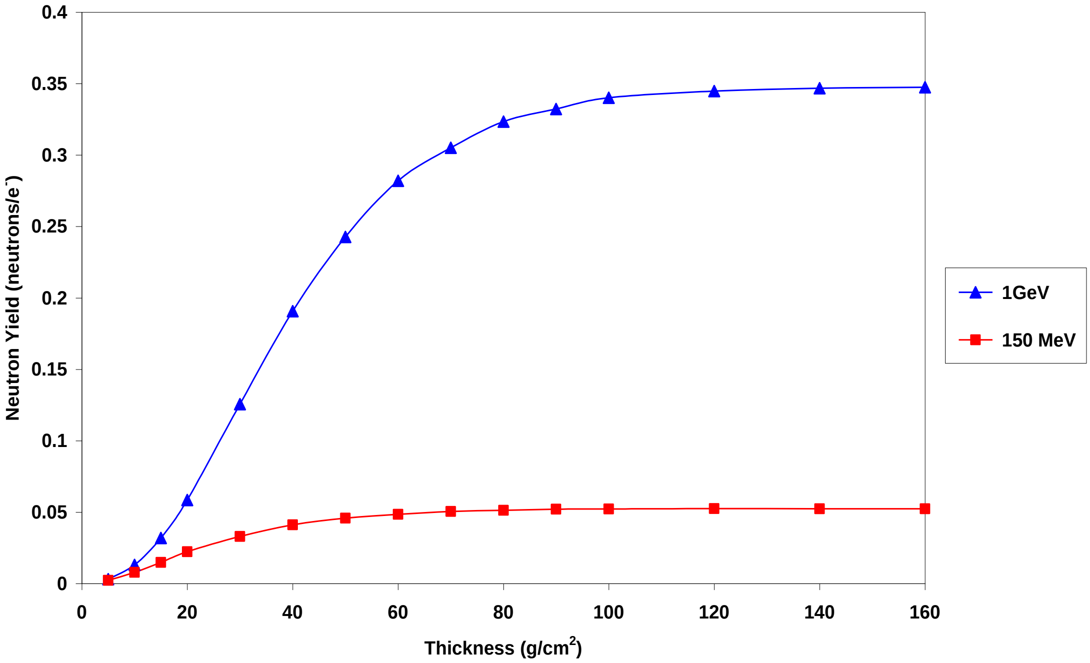

Figure 3: Neutron yield as function of target thickness for 1 GeV and 150 MeV energy electron incidents on Tungsten targets.

It is observed from figure 2 that as the target thickness increases, the neutron yield increases and saturates beyond the optimized thickness 7.28, 8.5 and 12.35 cm for Tungsten, Tantalum and Lead respectively. Tungsten produces higher photo-neutrons yield than Tantalum and Lead ***(Wasilewski & Wronka; 2006)***. From figure 3, as the energy of incident electrons increases, the neutrons yield shows significant increase. The observed increase in neutrons yield may be attributed to the increase of "useful" photons fraction, i.e. photons have energy greater than the binding energy and lying in the GDR or QD ranges ***(Ridikas &et. al.; 2002)***. Also, due to the increase of electron photon cascaded showers that increase as the electron energy increases. The electron photon cascaded showers can induce photon multiplications in both GDR and QD energy regions. The optimized thickness and the maximum neutrons yield obtained from these targets are listed in table 1.

Table 1 the maximum neutrons yield at optimize thickness of Tungsten, Tantalum and Lead targets

Target	Electron beam energy	Max. Yield (neutrons/e^-)	Optimized thickness (g/cm^2)	Optimized thickness (cm)
Tungsten Z=74, ρ=19.24	1GeV	3.47×10^{-1}	140	7.28
	150MeV	5.23×10^{-2}	100	5.2
Tantalum Z=73, ρ=16.4	1GeV	3.2×10^{-1}	140	8.5
Lead Z=82, ρ=11.34	1GeV	2.98×10^{-1}	140	12.35

Figure 4 shows the forward neutron intensity in comparison with the neutron yield produced from 1GeV electron energies impinging on Tungsten target. From figure 4, it is observed that the majority of neutrons yield are emitted in the outward direction. Also, the neutrons yield emits in forward direction increase as the target thickness increase until certain thickness (60-70 g/cm^2) then decreases. At certain thickness (60-70 g/cm^2) almost 23% of the neutron yield is generates in forward direction.

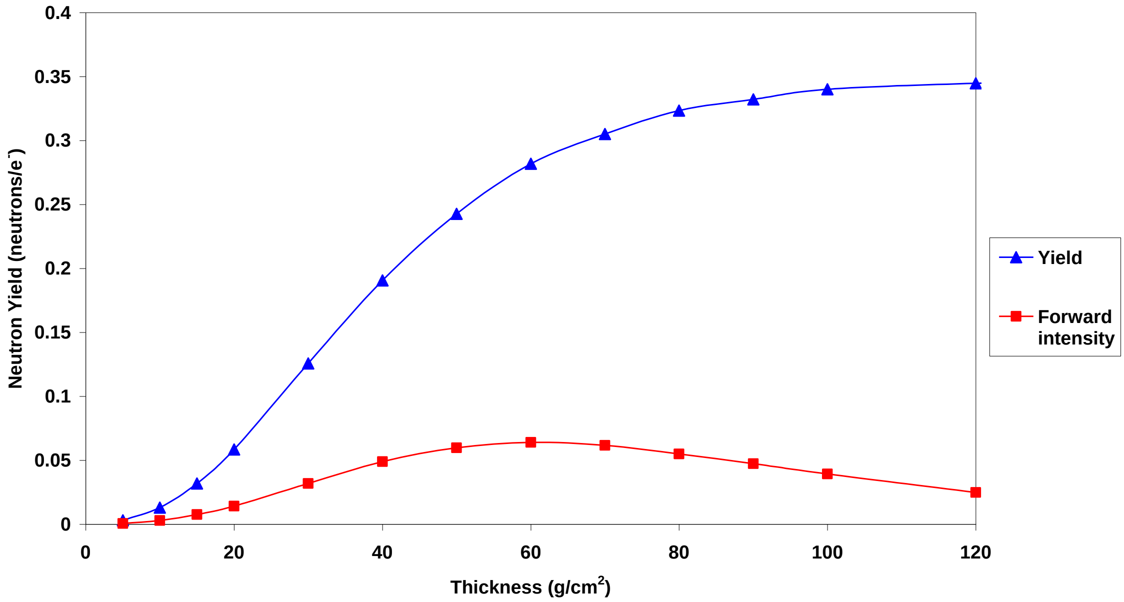

Figure 4: Neutron yield and forward neutron intensity as function of target thickness for 1 GeV energy electron incidents on Tungsten targets.

3.2 Angular distribution of photo-neutrons

Figure 4 shows the angular distribution of neutrons produced from 1 GeV and 150 MeV incident electrons on the optimized thickness of Tungsten target. Figure 6 represents the angular distribution of neutrons produced from 1 GeV incident electrons on different thicknesses of Tungsten.

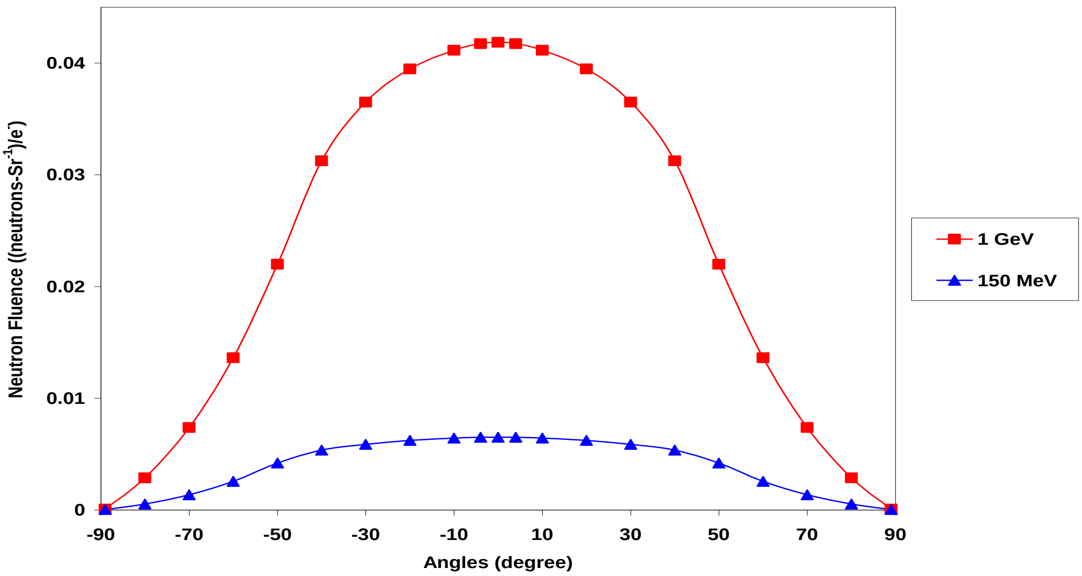

Figure 5: Angular distribution of neutrons as function of angle for 1 GeV and 150 MeV electron energy incidents on optimized thickness of Tungsten

From figure 5 it is noticed that as the energy of the incident electron decreases, the neutron fluence is almost isotropic ***(X-5 MCNP Team; 2003).*** The isotropic nature of neutrons is due to the dominance of GDR neutrons. The neutrons emitted by GDR mechanism is like the evaporation neutrons from a compound nucleus ***(Sahani &et. al.; 2012)***.

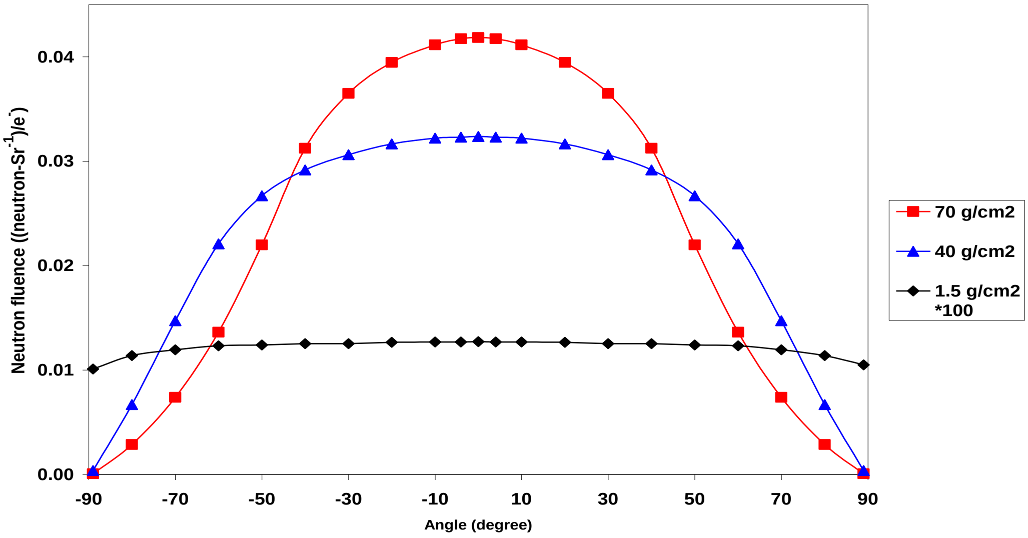

Figure 6: Angular distribution of neutrons as function of angle for 1 GeV electron energy incidents on different thickness of Tungsten.

From figures 6 it is observed that for thin targets the neutrons are produced in an isotropic form. As the target thickness increases the neutron fluence is assumed to be anisotropic for 1 GeV electrons. The noticed forward-peaked angular distributions may be attributed to the increase of Pre-equilibrium emission of neutrons ***(X-5 MCNP Team; 2003)*** by increasing the target thickness and due to the anisotropic emission of neutrons from the QD and Photo-Pion decay ***(Sahani &et. al.; 2012***). Such forward-peaked angular distribution can deliver the highest neutron fluence per cm^2 in forward direction (0 angle).

3.3 Energy spectrum

Figure 7 shows the energy distribution of neutrons generated from 1 GeV electron beams impinging on Tungsten, Tantalum and Lead targets respectively.

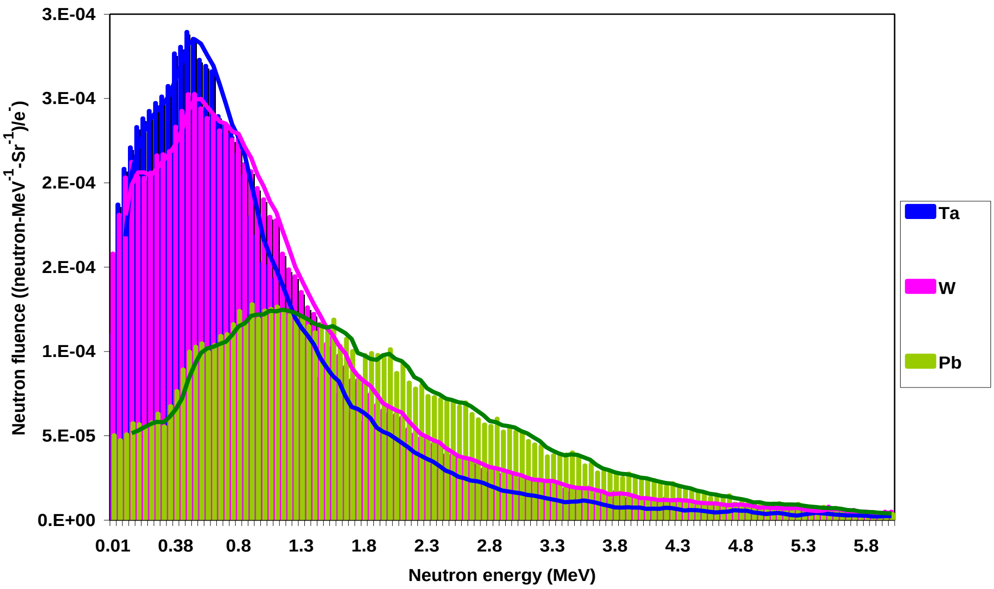

Figure 7: Energy distribution of neutrons produced from 1 GeV electrons incidents on 60g/cm^2 thickness of different targets.

From figure 7, the energy spectrum can be well described by a Maxwellian distribution, which is dominated by the low energy neutrons with peak at 0.6, 0.58, 1.2 MeV for Tungsten, Tantalum and Lead targets respectively. The fitted equation of the distribution ***(Petwal &et. al.; 2007)*** is:

$$\frac{dN}{dE_n} = k\frac{E_n}{T^2}\exp\left(\frac{-E_n}{T}\right) \qquad (2)$$

Here T is a nuclear temperature (MeV), which is characteristic of a particular target nucleus and represents the most probable energy of the generated neutrons, k is a normalization factor. From equation fitting the calculated values of the nuclear temperature T are 0.44, 0.57 and 0.98 MeV for Tungsten, Tantalum and Lead targets respectively ***(Swanson W. P.*; 1979)**. The high nuclear temperature value for Lead may be attributed to its high binding or neutron separation energy due to the existence of the magic number (82) in lead nucleus ***(Mao &et. al.; 1996)***.

3.4 Mean energy of photo-neutrons

The average mean energies of photo-neutrons are 1.64, 1.41 and 2.24 MeV for Tungsten, Tantalum and Lead targets respectively bombarded to 1 GeV electrons and 1.58 MeV for 1 50 MeV electrons impinging Tungsten. It is observed that Tantalum can produce neutrons with lower mean energy than that for Tungsten and Lead. The high mean energy of lead may be attributed to the high nuclear temperature (T) of Lead ***(Mao &et. al.; 1996)***.

4. Conclusion

As a conclusion, the photo-neutron yield increases as the target thickness increases then saturates beyond an optimized thickness of the target. Tungsten produces photo-neutrons more than Tantalum and Lead. Also, the photo-neutron yield shows significant increase as the electron energy increases. At the optimized thickness, the angular distribution of photo-neutrons is found almost isotropic for 150 MeV electrons and anisotropic for 1 GeV electrons. Further, by increasing the electron energy and/or the target thickness the angular distribution is found to be forward peaked. The energy spectrum of photo-neutrons can be well described by a Maxwellian distribution for both electron energies and the calculated values for nuclear temperature *T* are 0.44, 0.57 and 0.98 MeV for Tungsten, Tantalum and Lead targets respectively. Such calculations can help in developing a photo-neutron source based time of flight facility (TOF) for elemental and isotopic identification via neutron resonance spectroscopy.

5. References

Ban S., Namito Y., Hirayama H., Terunuma N., Urakawa J., Sato T., Yuasa R., Shin K., Lee H. S. and Bak J .S., (2000):Measurements of Photoneutron Spectra from Thick Pb Target Bombarded by 1.2 and 2.0 GeV Electrons,Proceedings of 2^{ed} International Workshop on EGS, Tsukuba, Japan, KEK Proceedings 200-20, Pp.130-134.

Brkic H., Ivkovic A., Kasabasic M., Sovilj M. P., Jurkovic S., Stimac D., Rubin O. and Faj D., (2016): The influence of field size and off-axis distance on photoneutron spectra of the 18 MV Siemens Oncor linear accelerator beam, Radiation Measurements, Vol. 93, Pp 28-34.

Hai-Bo X., Xian-Ke P. and Chao-Bin C., (2010): Monte Carlo simulation for bremsstrahlung and Photo neutron yields in high-energy x-ray radiography, Chin. Phys. B., Vol. 19, No. 6, 062901(1-8).

Junghans A., (2014): Neutron beams for nuclear data measurements, Neutrons and Nuclei, École Joliot-Curie (EJC), Fréjus, France.

Mao X., Kase K. R. and Nelson W. R., (1996): Giant Dipole Resonance neutron yields Produced by electrons as a function of target material and thickness, SLAC-PUB-6628.

***Patil B. J., Dhole S. D.,* (2010):** Studies on (i) Characterization of Bremsstrahlung spectra from High Z elements and (ii) Development of Neutron source using MeV pulsed electron beam and their applications, proceedings of the DAE symp. on nucl. Phys. 55.

Petwal V. C., Senecha V. K., Subbaiah K. V., Soni H. C. and Kotaiah S.,(2007): Optimization studies of photo-neutron production in high-Z metallic targets using high energy electron beam for ADS and transmutation, Pramana Journal of Physics, Vol. 68, No. 2, Pp 235-241.

Quintieri L., Bedogni R., Buonomo B., Esposito A., De Giorgi M., Mazzitelli G., Valente P. and Gomez -Ros J. M.**, **(2012): Photoneutron source by high energy electrons on high Z target: comparison between Monte Carlo code and experimental data, Transactions of fusion science and technology, Vol. 61, Pp314−421.

Ridikas D., Safa R., Giacri M. L.,(2002): Conceptual study of neutron irradiator driven by electron accelerator, 7th Information Exchange Meeting on Actinide and Fission Product P&T (NEA/OCDE), Jeju, Korea.

Sahani P. K., Haridas G., Sarkar P. K., (2012): simulation of photoneutron spectra due to incident high energy electrons on tungsten target using FLUKA, Indian Journal of Pure & applied physics, Vol. 50, pp. 863-866.

Swanson W. P., **(1979):** Radiological safety aspects of the operation of electron linear accelerators, IAEA T R, Technical Report Series No. 188, IAEA.

Wasilewski A. and Wronka S.**, **(2006): Monte-Carlo simulations of a neutron source generated with electron linear accelerator, Nukleonika, Vol. 51(3), Pp169−173.

X-5 MCNP Team, (2003): A general Monte Carlo N-Particle transport code, version 5, Los Alamos National Laboratory Report, LA-UR-03-1987.

Zolfaghari M. and Sedaghatizadeh M.**, **(2015): Design and Simulation of Photoneutron Source by MCNPX Monte Carlo Code for Boron Neutron Capture Therapy, Iranian Journal of Medical Physics (IJMP), Vol. 12, No. 2, Pp. 129-136.

خصائص النيوترونات الناتجة من فرمله الكترونات ذات طاقه 150 ميجا و 1 جيجا إلكترون فولت في أهداف معدنية ثقيلة للاستخدام في مطيافيه الرنين النيوتروني

الطيب السعدى ابراهيم [1]،مصطفى محمد مصطفى العشماوى[1]،حسنيه محمد ابو زيد[2]،عفاف احمد ندا [2]،فاطمه الزهراء محمد رجب[2]
1- هيئه الرقابه النوويه والاشعاعيه
2-كليه البنات للاداب والعلوم والتربيه –جامعه عين شمس

الملخص

تم استخدام كود مونت كارلو لحساب كميه النيوترونات والتوزيع الزاوي وطيف الطاقة الناتجة من فرمله الكترونات ذات طاقه 1 جيجا إلكترون فولت و 150 ميجا إلكترون فولت في أهداف من التنجستين و التنتاليوم والرصاص. وقد لوحظ من هذه الدراسة أن كميه النيوترونات الناتجة تزداد بزيادة سمك الهدف المستخدم وعند سمك مثالي فإن كميه النيوترونات الناتجة لا تتأثر بأي زيادة إضافية في سمك الهدف. كما تبين أن كميه النيوترونات الناتجة تزداد بشده بزيادة طاقة الالكترونات الساقطة على الأهداف. وعند سمك المثالي للهدف فإن التوزيع الزاوي للنيوترونات اظهر توزيعا متماثل في حاله الكترونات ذات الطاقة 150 ميجا إلكترون فولت و توزيعا غير متماثل في حاله الكترونات ذات الطاقة 1 جيجا إلكترون فولت.و بزيادة طاقه الالكترونات أو بزيادة سمك الهدف فإن التوزيع الزاوي يظهر مزيد من التحدب في الاتجاه الأمامى . تبين أيضا أن طيف طاقه النيوترونات الناتجة يمكن وصفه بتوزيع ماكسويل لكلا من الطاقتين المستخدمتين.هذه الحسابات يمكن أن تساعد في تطوير أليه زمن الطيران لقياس نسبه العناصر والنظائر باستخدام مطيافيه الرنين النيوتروني.